Inorganic Chemistry
Cite This: Inorg. Chem. XXXX, XXX, XXX–XXX
Forum Article
pubs.acs.org/IC

Time-Resolved Terbium-Based Probe for the Detection of Zinc(II) Ions: Investigation of the Formation of a Luminescent Ternary Complex

Matthew R. Winnett, Parvathy Mini, Michael R. Grace, and Kellie L. Tuck*

School of Chemistry, Monash University, Clayton, Victoria 3800, Australia

Supporting Information

ABSTRACT: Because of their unique photochemical and photophysical properties, luminescent lanthanide-based complexes have long captivated chemists. In recent years, the number of reports of luminescent lanthanide complex-based probes for monitoring of biological and environmental processes has dramatically increased, namely, because of their selectivity for particular analytes, lower limits of detection, and the fact that they allow monitoring of analytes in real time. Lanthanide-based probes need to be paired with an appropriate antenna/sensitizer to allow maximum energy transfer, with the antenna typically covalently attached to the stable lanthanide chelate. We have recently investigated "dark" lanthanide-based probes where the sensitizer is not covalently linked to the lanthanide chelate. Herein we report the use of a luminescent lanthanide-based probe system for the detection of Zn^{2+} ions based on the formation of a ternary complex between a "dark" terbium complex, lumazine, and Zn^{2+}. The terbium(III)-based probe incorporates a 1,4,7,10-tetraazacyclododecane-1,4,7,10-triacetic acid macrocyclic chelator covalently attached to a cyclen moiety, which is the Zn^{2+} ion binding group. In the presence of Zn^{2+} ions and lumazine (a strongly UV-absorbing sensitizer), a 1:1:1 ternary complex forms. The resulting complex is highly luminescent and selective for Zn^{2+} ions over other cations of environmental significance. Furthermore, with a limit of detection of 1.2 μM, this probe can detect the level of chronic zinc(II) concentrations denoted by the U.S. Environmental Protection Agency.

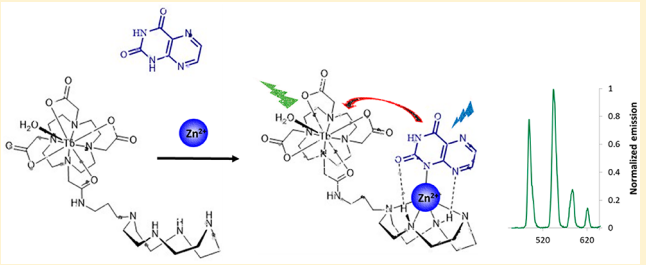

INTRODUCTION

In recent years, the total number of papers describing the development of luminescent, lanthanide complex-based sensors for monitoring of biological and environmental processes has dramatically increased (see refs 1−5 for recent reviews on the development of luminescent lanthanide-based probes). This is understandably due to their multiple advantages over organic dyes, which results from the unique photophysical properties of lanthanide ions. Lanthanide ions are weakly luminescent; however, when paired with a strongly UV-absorbing "antenna" group, indirect excitation can occur, resulting in narrow, well-defined emission bands, long emission lifetimes, and large Stokes shifts.[6] Figure 1a is a schematic representation of a lanthanide-based probe with a covalently attached antenna, although it is worth mentioning that transfer through space from a noncovalently attached antenna can also result in efficient energy transfer (ET; see later). The long, millisecond range, luminescent lifetimes of the resulting lanthanide emission allows background fluorescence to be removed via time-gated detection where a delay is set between the excitation pulse and the signal detection. Indirect excitation of the lanthanide ion occurs by excitation of the antenna from the ground state (S_0) to the singlet excited state (S_1); after intersystem crossing (ISC) to its triplet excited state (T_1), the lanthanide emission level is populated by ET from the antenna to the lanthanide (Figure 1b). Förster (through-space)[7−9] and Dexter (nonradiative)[10] ET mechanisms are possible. This sensitization process seems simplistic although various competing pathways may also occur, for example, vibrational relaxation, internal conversion, fluorescence, and ISC pathways.[11]

Two important considerations in the design of a luminescent lanthanide-based probe are (i) pairing of the lanthanide with an appropriate antenna to allow maximum ET and (ii) the formation of a stable lanthanide chelate to ensure that the lanthanide ion does not readily dissociate in solution. Some of the most commonly utilized lanthanide-ion-chelating ligands are shown in Figure 2, with 1,4,7,10-tetraazacyclododecane-1,4,7,10-triacetic acid (DOTA) and 1,4,7,10-tetraazacyclododecane-1,4,7-triacetic acid (DO3A) the most frequently used ligands because of the kinetic inertness and high thermodynamic stability of the corresponding lanthanide chelate. For these reasons, we have regularly used DOTA- or DO3A-based chelating ligands for the development of lanthanide-based probes.[12−19] Two recent examples from our group are the

Special Issue: Innovative f-Element Chelating Strategies

Received: June 14, 2019

DOI: 10.1021/acs.inorgchem.9b01771
Inorg. Chem. XXXX, XXX, XXX–XXX

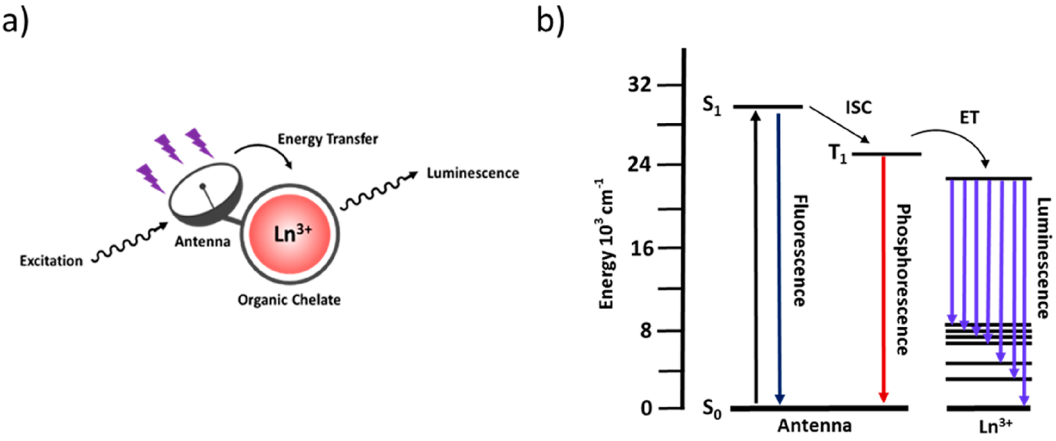

Figure 1. (a) Schematic representation of indirect excitation of the lanthanide ion due to the antenna effect. (b) Simplified Jablonski diagram that shows the pathway leading to lanthanide sensitization. Diagram modified and reproduced with permission from ref 1. Copyright 2018 Elsevier.

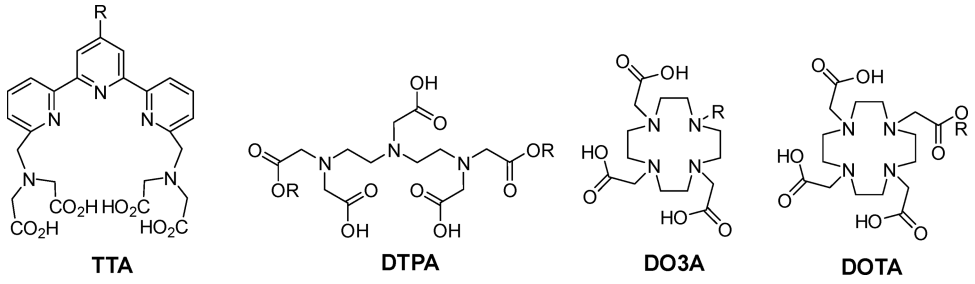

Figure 2. Chemical structures of common ligands used for chelating lanthanide ions.

terbium(III)-based complex (Figure 3a) featuring a Cu^{2+}-binding di-2-picolylamine (DPA) group and a pyridinyltriazole

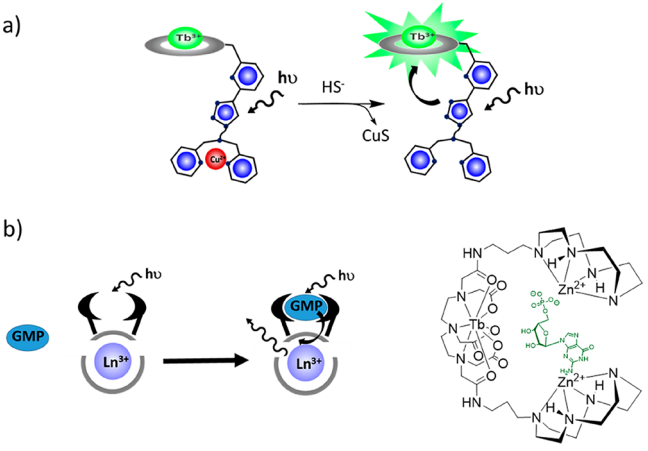

Figure 3. (a) Schematic representation of the HS^- sensing principle.[16] (b) Schematic representation of a "dark" lanthanide-based probe for the detection of GMP and the proposed model for binding of GMP to the trinuclear terbium(III)·zinc(II)$_2$ complex.[19]

antenna for the detection of hydrogen sulfide in aqueous solutions[16] and the "dark" trinuclear terbium(III)·zinc(II)$_2$ complex that is a luminescent sensor for the detection of guanosine phosphates in aqueous solutions.[19] A schematic representation and the proposed binding model for the detection of guanosine monophosphate (GMP) to the trinuclear terbium(III)·zinc(II)$_2$ complex are shown in Figure 3b.[19]

In the majority of examples of luminescent lanthanide-based probes, ours and others, the antenna has been covalently attached to the lanthanide chelate. More recently, we have been interested in the development of "dark" lanthanide-based probes in which the sensitizer is not covalently linked to the lanthanide chelate.[19] There are few examples of luminescent lanthanide-based probes of this type for the detection of analytes,[20] including one from our group.[19] These probes have minimal or no luminescence in the absence of the analyte, and a "turn-on" signal is observed upon binding of the analyte. For example, the trinuclear terbium(III)·zinc(II)$_2$ complex, shown in Figure 3b, which incorporates a diethylenetriaminepentaacetic acid chelating ligand and two cyclen moieties, is a luminescent sensor for the detection of guanosine phosphates in aqueous solutions but only upon formation of the required ternary complex.[19] Interaction occurs by the coordination of phosphate groups to the Zn^{2+} ions, and in this example, the guanine moiety is the antenna. Uridine also formed a noncovalent interaction with the cyclen–zinc(II) complex.[19]

For a number of years, we have investigated the development of fluorescent probes and luminescent lanthanide-based probes for the detection of Zn^{2+} ions.[12,21,22] Zn^{2+} ions are an essential micronutrient for the health and survival of plants, animals, and other organisms but are cytotoxic at high concentrations.[23] However, because Zn^{2+} ions have an electronic configuration of d^{10}, they are magnetically and spectroscopically inactive, which makes their detection challenging.[12] Previous probes for the detection of Zn^{2+} ions, from our group and others, have resulted in signal enhancement and quenching effects in the presence of Cd^{2+} and Cu^{2+} ions, respectively. Recent turn-on probes for Zn^{2+} ions are the previously mentioned sensors from the group of Sénèque,

DOI: 10.1021/acs.inorgchem.9b01771
Inorg. Chem. XXXX, XXX, XXX−XXX

which utilize an antenna grafted onto zinc finger peptides,[20] from Yuan and co-workers, which feature a DPA Zn^{2+} binding group,[24,25] and from Tripier and co-workers, which incorporate a 1,4,7-triazacyclononane Zn^{2+}-binding group.[26] Gunnlaugsson et al. reported a turn-off probe that contains a 8-hydroxyquinoline-5-sulfonic acid antenna that is displaced in the presence of Zn^{2+} ions.[27] On the basis of our recent success with the synthesis of ternary lanthanide-based complex for the detection of GMP, which utilized a cyclen−zinc(II) binding interaction, we were interested in applying this knowledge to develop a ternary luminescent lanthanide-based probe for the detection of Zn^{2+} ions. It has been shown, using density functional theory calculations, that the stabilization energy of thymine binding to the M^{2+}−cyclen complex follows the order $Zn^{2+} > Cu^{2+} > Ni^{2+}$ (Figure 4a) because of the stronger charge transfer from the anionic nitrogen to the metal.[28] Han and Kim have investigated the use of lumazine, a nitrogen-containing heterocycle that contains an imide functional group and a cyclen unit for the detection of Zn^{2+} ions.[29] A fluorescent "turn-on" effect is observed in the presence of 1 equiv of cyclen, lumazine, and Zn^{2+} ions (Figure 4b). The cyclen−lumazine complex was selective for Zn^{2+} over Cd^{2+} ions (a 14% increase in the fluorescence intensity observed for Cd^{2+}) and Cu^{2+} ions (minimal quenching observed), although competition studies in the presence of Zn^{2+} ions were not conducted. It was established, by X-ray crystallographic structural analysis, that the binding of Zn^{2+} to lumazine occurs at the N1 position, as shown in Figure 4b.[29]

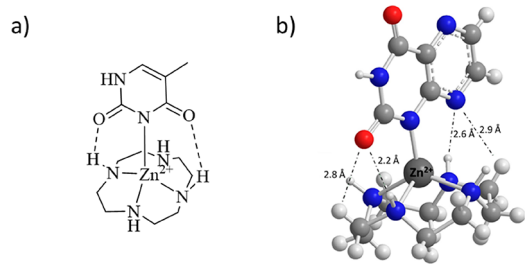

Figure 4. (a) Formation of the cyclen−zinc(II)−thymine ternary complex. (b) Drawing of the X-ray crystal structure of the cyclen−zinc(II)−lumazine complex, CSD Entry GUVFUY (coordinates obtained from CCDC and ref 29).

From our previous studies[13,19] and the work of Han and Kim,[29] we proposed that Tb-**1** (Figure 5) could be used to detect Zn^{2+} ions selectively over other cations in the presence of 1 equiv of lumazine. Herein we disclose the synthesis and analysis of a terbium-based ternary sensor for the detection of Zn^{2+} ions in aqueous solutions. The antenna, lumazine, forms a 1:1:1 adduct with Tb-**1** in the presence of Zn^{2+} ions. In Tb-**1**, the Zn^{2+} ion binding group, a cyclen moiety, is connected via a covalent linker to the lanthanide chelate (Figure 5). The addition of Zn^{2+} ions will result in the formation of a ternary cyclen−zinc(II)−lumazine complex, thereby positioning lumazine in close proximity to the terbium(III) center; hence, ET is now possible, culminating in a "turn-on" of luminescence. It was hoped that this rationally designed ternary complex would have a superior selectivity profile for Zn^{2+} ions because of this 3-point metal-ion-recognition motif compared to those previously published.

RESULTS AND DISCUSSION

Synthesis of Tb-1. The DOTA-based ligand was synthesized according to Scheme 1. Installation of the aminopropyl linker was achieved by a two-step procedure, alkylation of the tri-Boc-protected cyclen **2** (Boc = *tert*-butoxycarbonyl) with *N*-(3-bromopropyl)phthalimide, followed by cleavage of the phthalimide group with hydrazine, resulting in formation of the Boc-protected primary amine **3**. The reaction of this primary amine **3** with the tri-Boc-protected DOTA-carboxylic acid **4** [see the Supporting Information (SI) for the synthesis], initially activated as *N*-hydroxysuccinimide ester, gave the coupled product **5**. Global deprotection, under acidic conditions, gave ligand **1**, which was purified by preparative reverse-phase high-performance liquid chromatography (RP-HPLC) and isolated as a trifluoroacetate salt. The terbium complex Tb-**1** was obtained after reaction of the ligand with $Tb(CF_3SO_3)_3$ and heating of the reaction mixture overnight. Purification by preparative RP-HPLC gave the terbium(III) complex as a trifluoroacetate salt.

Characterization of Tb-1 as a Luminescent-Based Lanthanide Sensor for Zn^{2+}. As expected, because of the

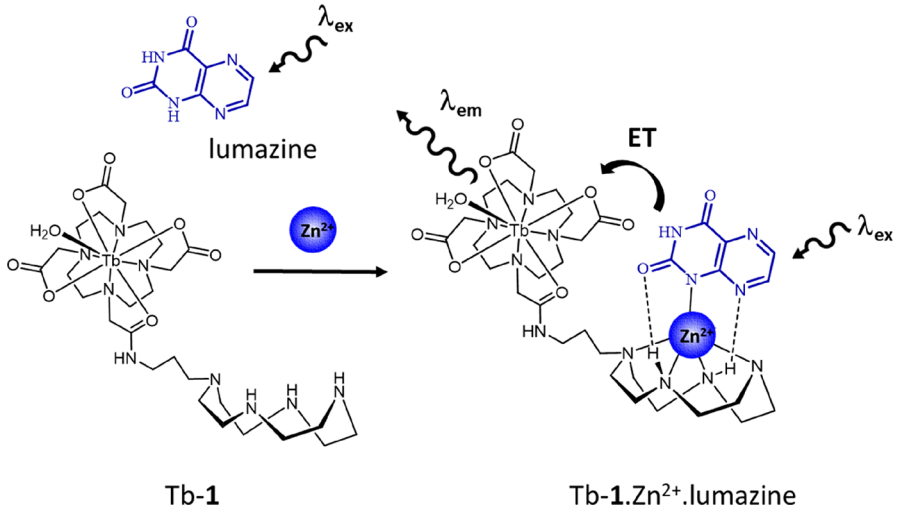

Figure 5. Schematic of the "dark" lanthanide-based probe Tb-**1**, which contains a cyclen−zinc(II) binding moiety. In the presence of lumazine, a luminescent increase will be observed, which is directly proportional to the concentration of Zn^{2+} ions.

DOI: 10.1021/acs.inorgchem.9b01771
Inorg. Chem. XXXX, XXX, XXX−XXX

Scheme 1. Synthesis of Tb-1

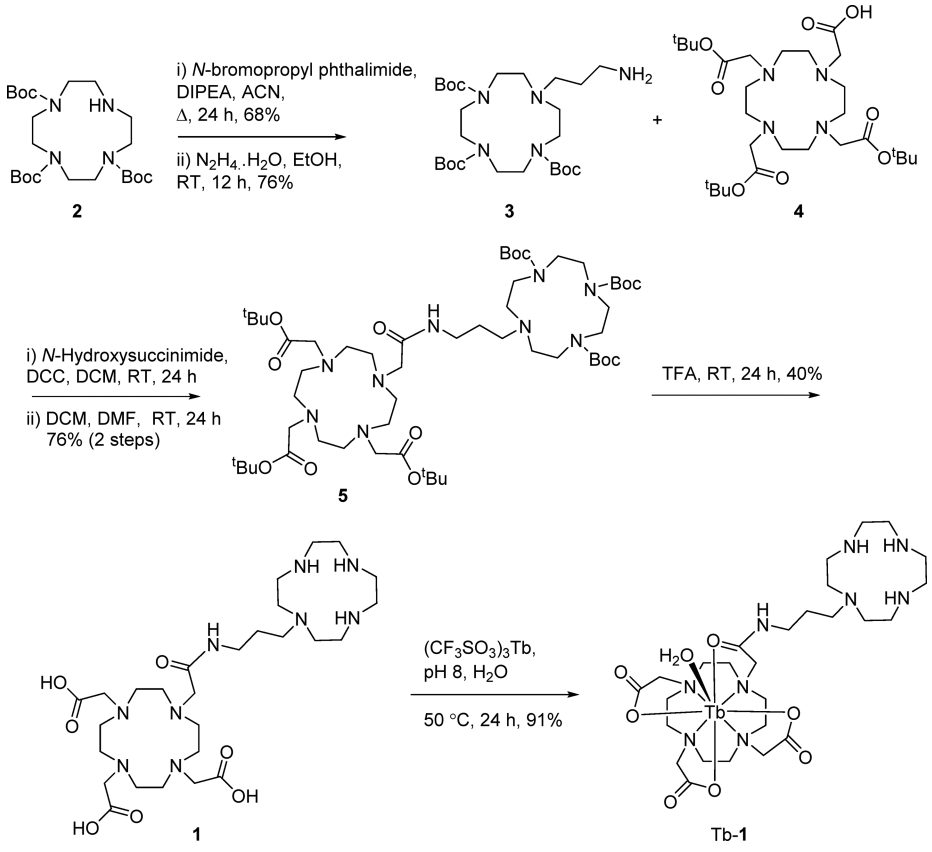

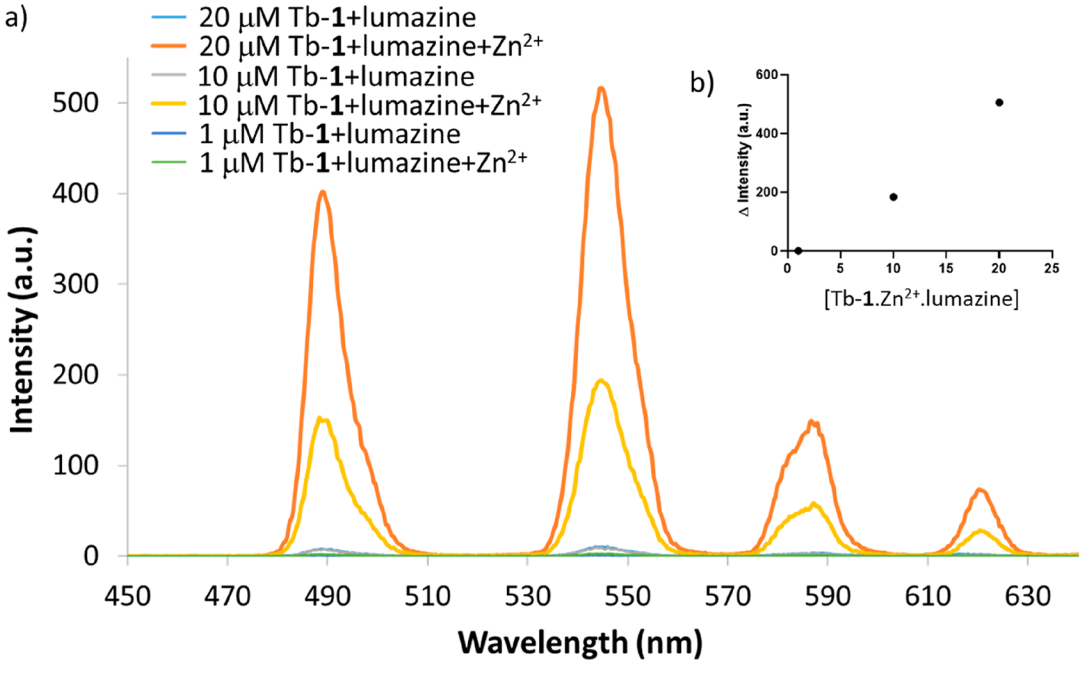

Figure 6. (a) Time-delayed emission spectra (λ_{ex} = 325 nm) of Tb-**1** + lumazine at different concentrations (1, 10, and 20 μM) with and without the addition of 1 equiv of Zn^{2+}. (b) Difference in the luminescent intensity changes detected at 545 nm for Tb-**1**·Zn^{2+}·lumazine complexes. All spectra were measured in a 10 mM HEPES buffer (pH 7.4).

absence of an appropriate sensitizer, time-resolved luminescent analysis of the complex Tb-**1**, in a 10 mM 4-(2-hydroxyethyl)-piperazine-1-ethanesulfonic acid (HEPES) buffer at pH 7.4, revealed that it was not luminescent. Upon the addition of 1 equiv of lumazine and 1 equiv of Zn^{2+} ions, four distinct bands corresponding to transitions from the $^5D_4$ excited state to the $^7F_6$, $^7F_5$, $^7F_4$, and $^7F_3$ ground states were observed in the luminescence spectrum, with emission maxima at 489, 545,

DOI: 10.1021/acs.inorgchem.9b01771
Inorg. Chem. XXXX, XXX, XXX−XXX

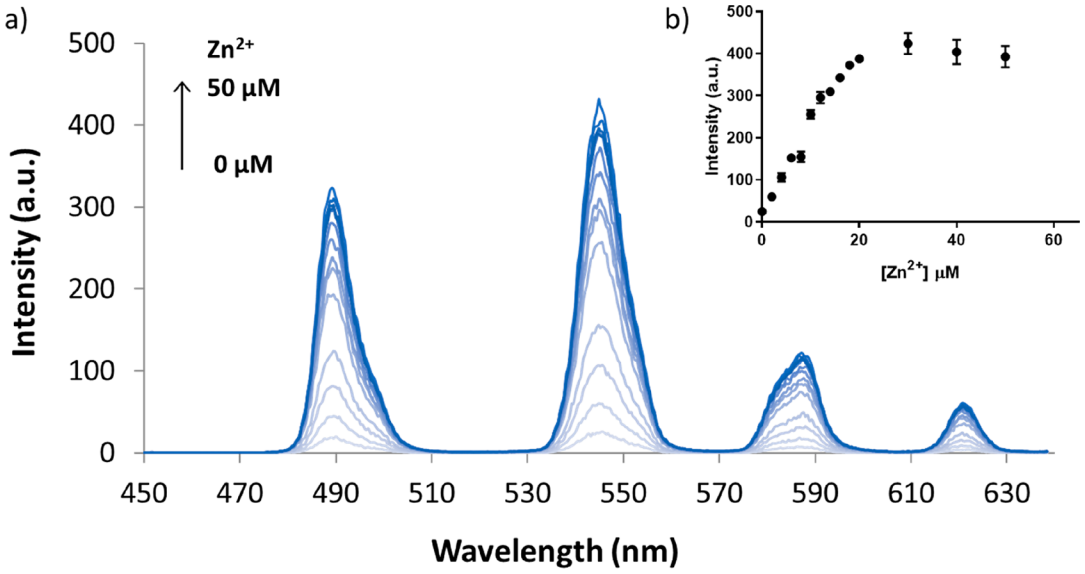

Figure 7. (a) Time-delayed emission spectra (λ_{ex} = 325 nm) of Tb-**1** (20 μM) and lumazine (20 μM) with the addition of various amounts of Zn^{2+} (0−50 μM). (b) Luminescent intensity changes detected at 545 nm. Spectra were measured in a 10 mM HEPES buffer (pH 7.4) and show the average of triplicate results (n = 3).

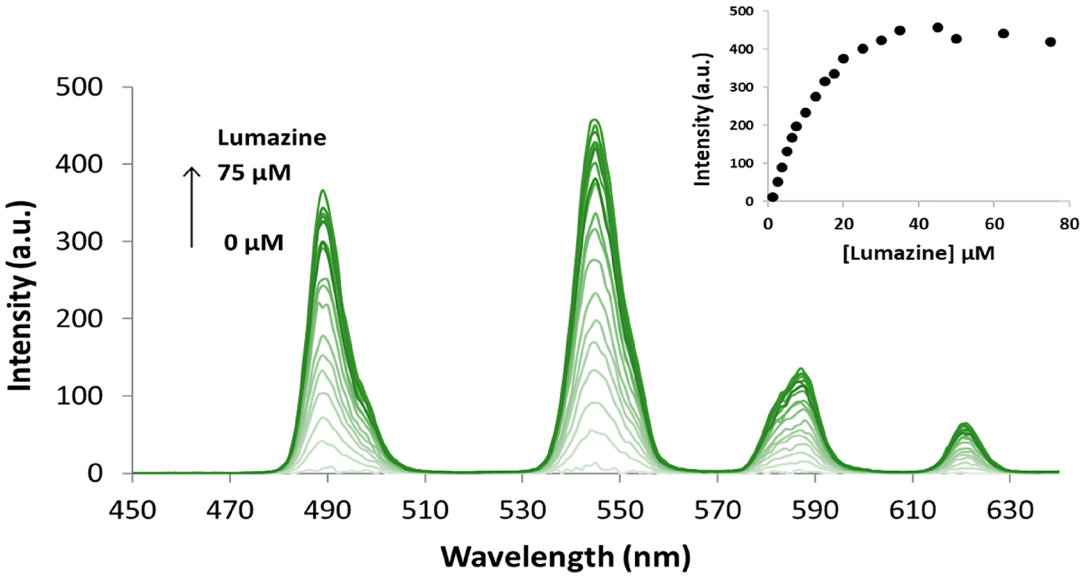

Figure 8. (a) Time-delayed emission spectra (λ_{ex} = 325 nm) of Tb-**1** (20 μM) and Zn^{2+} (20 μM) with the addition of various amounts of lumazine (0−75 μM). (b) Luminescent intensity changes detected at 545 nm. Spectra were measured in a 10 mM HEPES buffer (pH 7.4).

587, and 620 nm, respectively (Figure 6a). The increase in luminescence in the presence of lumazine and Zn^{2+} ions can be attributed to the sensitizing capability of lumazine; this can be observed from the excitation spectrum of Tb-**1**·Zn^{2+}·lumazine (Figures S1 and S2). The ET is surmised to occur via through-space Förster ET, where the efficiency of ET is inversely proportional to the sixth power of the distance between the donor and acceptor. Hence, if the ternary adduct does not form, then ET is minimal and no luminescent emission is observed. Thus, in the absence of Zn^{2+} ions, but in the presence of Tb-**1** and lumazine, minimal luminescence is observed because of the absence of the cyclen−Zn^{2+} complex that is required for complexation of lumazine. Furthermore, it was observed that Tb-**1**·Zn^{2+} was not luminescent. All experiments were performed in an aqueous HEPES buffer at pH 7.4, and it was noted that at pH < 7 the solution containing Tb-**1** + Zn^{2+} + lumazine was weakly luminescent; this is presumably due to formation of the Tb-**1**·Zn^{2+}·lumazine ternary adduct being unfavorable below the pK_a value of lumazine because one of the imide protons of lumazine needs to be deprotonated to facilitate formation of the ternary adduct (Figure 5). The optimum concentration of the 1:1:1 ternary adduct Tb-**1**·Zn^{2+}·lumazine was investigated at three concentrations (1, 10, and 20 μM), with the 20 μM Tb-**1**·Zn^{2+}·lumazine adduct, understandably, giving the greatest signal-to-noise ratio (Figure 6).

The luminescent intensity of a 1:1 mixture of Tb-**1** (20 μM) and lumazine (20 μM) increases ca. 20-fold upon the addition of 1 equiv of Zn^{2+} ions, before reaching saturation, and a linear response was observed over the concentration range 0−18 μM Zn^{2+} (Figure 7). The luminescent signal was found to stabilize after 3 min, and the limit of detection (LoD) was 1.2 μM.

DOI: 10.1021/acs.inorgchem.9b01771
Inorg. Chem. XXXX, XXX, XXX−XXX

Table 1. Binding Models for the Host–Guest Interaction, Determined Using supramolecular.org[34],[a]

host	guest	binding model (host–guest)	K_1 (M^{-1})	K_2 (M^{-1})
Tb-**1**·Zn^{2+} (20 μM)	lumazine (↑)	1:1	2.6×10^6 M^{-1} ± 7.8%	
Tb-**1** (20 μM)	lumazine (20 μM) + Zn^{2+} (↑)	1:2	1.0×10^7 M^{-1} ± 7.1%	3.1×10^5 M^{-1} ± 7.8%
Tb-**1** (5 μM)	lumazine (5 μM) + Zn^{2+} (↑)	1:2	5.0×10^6 M^{-1} ± 4.7%	3.3×10^5 M^{-1} ± 5.1%

[a] λ_{ex} = 325 nm; (↑) denotes increasing guest concentration.

Time-gated experiments were separately performed with Tb-**1** (5 μM) and lumazine (5 μM); a similar increase in luminescence was observed with a plateau at ca. 1 equiv of Zn^{2+} ions (Figure S3). The number of inner-shell-coordinated water molecules (q) present upon formation of the 1:1:1 Tb-**1**·Zn^{2+}·lumazine ternary adduct was determined by measuring the emission lifetimes of the ternary adduct in H_2O and D_2O, respectively.[30] The DOTA analogue provides eight coordination sites for the terbium(III) center, and the ninth site is occupied by the bound water molecule.

The change in the luminescent intensity upon the addition of lumazine to a 1:1 mixture of Tb-**1** (20 μM) and Zn^{2+} ions (20 μM) was investigated (Figure 8). Upon the addition of 1 equiv of lumazine, an increase of ca. 380-fold in the luminescent intensity was observed, and only small changes to the luminescent intensity occurred after the addition of 1.5 equiv of lumazine. A 5 min incubation time was necessary to ensure complete formation of the ternary adduct.

Binding Mode for Formation of the Ternary Adduct Tb-1·Zn^{2+}·Lumazine. As previously noted,[20] the Job plot method has been deemed unsuitable for stoichiometric determination in supramolecular events, and it is desirable to fit the data obtained from titration studies.[31−33] supramolecular.org,[34] an Open Access program, was utilized to investigate the binding of Zn^{2+} ions to Tb-**1** + lumazine at two different concentrations (5 and 20 μM), with the binding of lumazine to the Tb-**1**·Zn^{2+} complex also investigated. Three different binding modes corresponding to host–guest interactions (1:1, 1:2, or 2:1) were analyzed using data from the respective titration experiments (λ_{ex} = 325 nm; Table 1). In the case where the host is the preformed Tb-**1**·Zn^{2+} complex and the guest was lumazine, the 1:1 binding model resulted in an acceptable fit with low (co)variance of the fit. In the cases of Tb-**1** + lumazine and increasing concentrations of Zn^{2+} (5 and 20 μM), a 1:2 host–guest resulted in the most acceptable fit. It is noted here that, because Tb-**1** + lumazine does not form a preformed complex, it is thus assumed that Tb-**1** is the host, where the first guest is Zn^{2+} ions and the second guest is lumazine.

Selectivity of Tb-1 + Lumazine for Zn^{2+} Ions. It is possible that other environmentally relevant cations (M) could assist in the formation of a ternary adduct [Tb-**1**·(M)·lumazine]. Hence, the luminescent response of Tb-**1** in the presence of lumazine and various cations (1 and 10 equiv of Mg^{2+}, Na^+, Hg^{2+}, Ca^{2+}, Cd^{2+}, Co^{2+}, Cu^{2+}, Ni^{2+}, K^+, and Fe^{3+}) was investigated (Figure 9). It was hoped that we would not see as great a luminescent increase upon the addition of Cd^{2+} ions as that for Zn^{2+} ions. Unfortunately, this was not the case, and the addition of 1 equiv of Cd^{2+} ions resulted in almost the same luminescent increase as that with the addition of 1 equiv of Zn^{2+} ions. As expected, the addition of 1 equiv of other cations (Mg^{2+}, Na^+, Hg^{2+}, Ca^{2+}, Co^{2+}, Cu^{2+}, Ni^{2+}, K^+, and Fe^{3+}) resulted in a minimal or no increase in luminescence (Figure 9a), therefore indicating that these cations are incapable of forming the ternary adduct that brings the strongly UV-absorbing lumazine moiety close in space to the terbium(III) ion; in the case of the paramagnetic ions, these ions quench the S_1 state of lumazine, preventing ET to the terbium(III) center. In all cases, except when the ion was Cu^{2+}, acceptable restoration of luminescence was observed. This suggests that the Cu^{2+} ions are binding to the cyclen moiety of the terbium(III) complex and the Zn^{2+} ions are not able to displace them within the time frame of the experiment. Interestingly, in the case of the Ni^{2+} ions, which are also paramagnetic, full luminescent enhancement was observed upon the addition of Zn^{2+} ions. This indicates that either the Ni^{2+} ions did not bind to the cyclen moiety in the first place or the Zn^{2+} ions are able to readily displace the Ni^{2+} ions from the cyclen moiety. In our previous studies, we observed that, with a DPA moiety as the Zn^{2+} chelator, both Cu^{2+} and Ni^{2+} ions were competitive with the Zn^{2+} ions, resulting in a quenching effect.[12,22] In that case, Ni^{2+} bound more strongly than Zn^{2+} ions to the DPA unit and deactivated the excited state of the

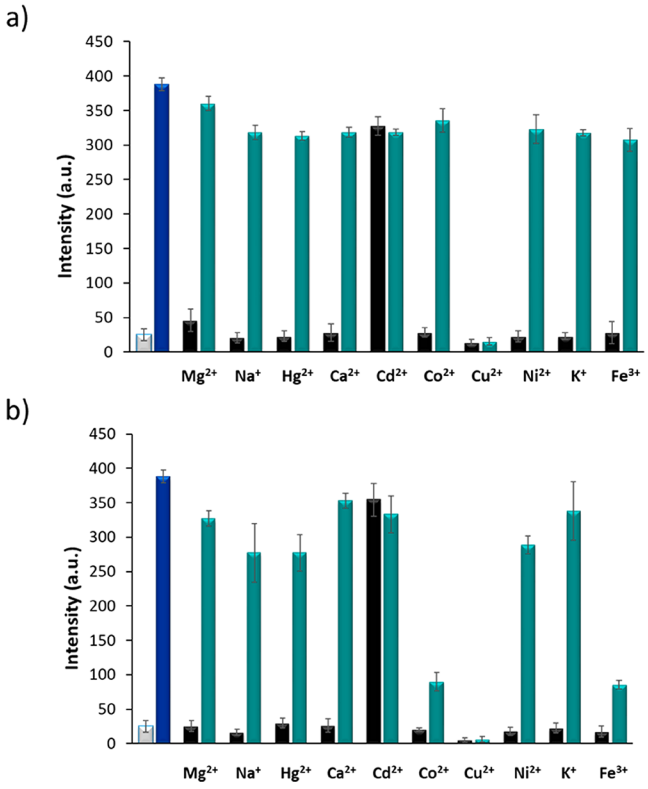

Figure 9. (a) Time-delayed emission spectra (λ_{ex} = 325 nm and λ_{em} = 545 nm) of Tb-**1** (20 μM) in the presence of various cations: gray bars, Tb-**1** (20 μM) + lumazine (20 μM); blue bars, Tb-**1** (20 μM) + lumazine (20 μM) + Zn^{2+} (20 μM) (a) Color code: black bars, Tb-**1** (20 μM) + lumazine (20 μM) + cation (20 μM); green bars, Tb-**1** (20 μM) + lumazine (20 μM) + cation (20 μM) + Zn^{2+} (20 μM). (b) Color code: black bars, Tb-**1** (20 μM) + lumazine (20 μM) + cation (200 μM); green bars, Tb-**1** (20 μM) + lumazine (20 μM) + cation (200 μM) + Zn^{2+} (20 μM) (n = 3).

DOI: 10.1021/acs.inorgchem.9b01771
Inorg. Chem. XXXX, XXX, XXX−XXX

terbium(III) center through intramolecular ET. The inclusion of a cyclen moiety, in the current design, therefore represents an improvement in our previous designs, allowing for the selective detection of Zn^{2+} ions in the presence of Ni^{2+} ions.

The addition of 10 equiv of these cations to Tb-**1** + lumazine produced a similar, more pronounced, effect, with the exception of Co^{2+} and Fe^{3+} ions, which resulted in quenching of the luminescence (Figure 9b). It was observed that the addition of various cations (1 and 10 equiv of Mg^{2+}, Na^{+}, Hg^{2+}, Ca^{2+}, Cd^{2+}, Co^{2+}, Cu^{2+}, Ni^{2+}, K^{+}, and Fe^{3+}) to a 5 μM solution of the ternary adduct, Tb-**1**·Zn^{2+}·lumazine, resulted in minimal luminescence intensity changes (Figure 10). Encouragingly, for

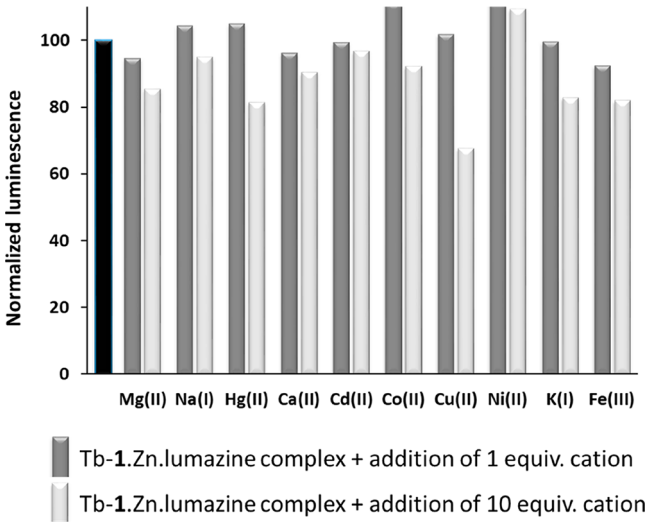

Figure 10. Normalized luminescence of the time-delayed emission spectra (λ_{ex} = 325 nm and λ_{em} = 545 nm) of Tb-**1** (5 μM) + Zn^{2+} (5 μM) + lumazine (5 μM) in the presence of various cations: black bar, Tb-**1**·Zn^{2+}·lumazine (5 μM); dark-gray bars, Tb-**1**·Zn^{2+}·lumazine (5 μM) + cation (5 μM); light-gray bars, Tb-**1**·Zn^{2+}·lumazine (5 μM) + cation (50 μM).

both analyses (Figures 9 and 10), the cations Mg^{2+}, Na^{+}, Ca^{2+}, and K^{+}, which are the most prevalent in aquatic environments, had minimal effect on the lanthanide emission of the Tb-**1**·Zn^{2+}·lumazine adduct.

We have shown that lumazine binds to Tb-**1**·Zn^{2+} with an association constant of 2.6×10^{6} M^{-1} ± 7.8%, and thus interference from anionic species such as nitrate, sulfate, and halide ions is expected to be minimal. However, there is the potential for interferences by (poly)phosphate-containing species because of the relatively high affinity of the phosphate moiety for mono(cyclen–Zn^{2+}) complexes (ca. 10^{3} M^{-1})[35,36] and bis(cyclen–Zn^{2+}) complexes (ca. 10^{6}).[19,36]

CONCLUSIONS

Two major challenges in the design of luminescent probes is to ensure that they are selective for the analyte of interest and are sufficiently sensitive for the application. Previously, luminescent lanthanide-based probes for the detection of Zn^{2+} ions have exhibited a turn-on response in the presence of Cd^{2+} ions and a quenching effect in the presence of Cu^{2+} and Ni^{2+} ions. Our rational design of a lanthanide-based ternary adduct possessing a 3-point binding interaction with Zn^{2+} ions showed improved selectivity for Zn^{2+} over Ni^{2+} ions compared to previous generations. However, interferences from Cd^{2+} and Cu^{2+} ions were still observed. The United States Environmental Protection Agency (U.S. EPA) ranks zinc as a priority pollutant with chronic zinc(II) concentrations noted as >1.84 μM for freshwater;[37] our sensor with a LoD (1.2 μM) can detect this threshold of Zn^{2+} ions. Additionally, the time-gated luminescence detection method is advantageous because it allows removal of the fluorescent background, making this sensor attractive for environmental or biological analyses.

Excitingly, we have contributed to the discovery of a novel "dark" lanthanide-based probe in which the sensitizer is not covalently linked to the lanthanide chelate. Because of the complete absence (darkness) of lanthanide emission in the absence of analyte, we believe that this subset of lanthanide-based probes has a key role to play in the detection of analytes in environmental systems.

EXPERIMENTAL SECTION

Material and Methods. All chemicals were purchased from either Merck or Sigma-Aldrich and used without purification. Compounds **2**[38] and **4**[39] were synthesized by modification of reported literature procedures. Flash chromatography was performed using Merck 38 silica gel 60, 230–400 mesh ASTM. Thin-layer chromatography (TLC) was performed on Merck silica gel 60 F254 plates. TLC plates were visualized using a UV lamp at 254 nm or through the use of a vanillin, $KMnO_4$, or ninhydrin staining agent. Preparative HPLC was performed on an Agilent Technology 1260 Infinity Prep LC controller with an Agilent 1260 Infinity Absorbance detector using a Phenomenex Luna C8 column (21.2 × 150 mm, 5 μm) with a 10 mL min^{-1} flow rate and 100% buffer A for 4 min and then a gradient from 100% buffer A to 100% buffer B over 30 min, where buffer A = 0.1% trifluoroacetic acid (TFA) in Milli-Q water and buffer B = 0.1% TFA in 80% acetonitrile (ACN)/20% Milli-Q water. ^{1}H NMR spectra were recorded on a Bruker DRX400 spectrometer operating at 400 MHz unless otherwise stated, as solutions in deuterated solvents as specified. Each resonance was assigned according to the following convention: chemical shift, multiplicity, observed coupling constants (J in hertz), and number of protons. ^{13}C JMOD NMR spectra were recorded on a Bruker DRX400 spectrometer operating at 100 MHz unless otherwise stated, as solutions in deuterated solvents as specified. Chemical shifts (δ), measured in parts per million (ppm), are reported relative to the residual proton peak in the solvent used as specified. High-resolution mass spectrometry (HRMS) was conducted using a Bruker BioApex 47e Fourier transform mass spectrometer fitted with an analytical electrospray ionization (ESI) source using NaI for accurate mass calibration. Low-resolution mass spectrometry (LRMS) was conducted using a Micromass Platform II quadrupole mass analyzer (ESI). IR spectra were recorded on an Agilent Technologies Cary 630 Fourier transform infrared spectrometer as thin films of compressed powders. UV–visible absorption spectra were recorded at room temperature using a Varian Cary 1E UV–visible spectrophotometer. A cell with a path length of 10 mm was used. Phosphorescence emission spectra were recorded at 22 °C using a Varian Cary-Eclipse fluorescence spectrophotometer. A quartz cell with a path length of 10 mm and a volume of 500 μL was used. Excitation and emission slit widths were both set at 5 nm, the delay time was 0.1 ms, and the gate time was 1 ms.

Syntheses. *1,4,7-Tri-tert-butoxycarbonyl-10-(3-propylamine)-1,4,7,10-tetraazacyclododecane (**3**).* Tri-Boc-cyclen **2** (BOC = *tert*-butoxycarbonyl;[36] 150 mg, 0.32 mmol), *N*-(3-bromopropyl)-phthalimide (85 mg, 0.63 mmol), and *N*,*N*-diisopropylethylamine (55 μL, 0.38 mmol) were dissolved in ACN (5 mL). The reaction mixture was heated to reflux for 24 h. After removal of the solvent in vacuo and purification by silica gel chromatography (35% ethyl acetate in poly(ethylene terephthalate); R_f = 0.3), the phthalimide (tri-*tert*-butyl 10-[3-(1,3-dioxoisoindolin-2-yl)propyl]-1,4,7,10-tetraazacyclododecane-1,4,7-tricarboxylate) was obtained as a clear oil (140 mg, 68%). ^{1}H NMR ($CDCl_3$): δ 1.41 (s, 18H), 1.46 (s, 9H), 1.86 (p, J = 7.3 Hz, 2H), 2.62 (m, 6H), 3.24–3.53 (broad m, 12H), 3.69 (t, J = 7.0 Hz, 2H), 7.72 (m, 2H), 7.84 (m, 2H). IR (ATR): 2974, 2931,

DOI: 10.1021/acs.inorgchem.9b01771
Inorg. Chem. XXXX, XXX, XXX–XXX

2814, 1673, 1459, 1409, 1364, 1245, 1148, 1088, 772 cm^{-1}. LRMS (ESI). Calcd for $[M + H]^+$: m/z 660.4 (100%). HRMS (ESI). Calcd for $[M + H]^+$: m/z 660.3976. Found: m/z 660.3976.

The phthalimide (300 mg, 0.46 mmol) was dissolved in ethanol (15 mL), hydrazine monohydrate (0.2 mL) was added, and the solution was stirred at ambient temperature. After 24 h, H_2O (2 mL) was added and ethanol was removed in vacuo. After the addition of 10% NH_4OH (10 mL) and extraction with $CHCl_3$ (3 × 30 mL), the combined organics were dried using $MgSO_4$ and concentrated in vacuo to obtain the title compound as a white solid (169 mg, 76%). HRMS (ESI). Calcd for $[M + H]^+$: m/z 530.3912. Found: m/z 530.3916. All spectral data were consistent with that previously published.[20]

*10-[1,4,7-Tri-tert-butoxycarbonyl-10-(propylamino)-1,4,7,10-tetraazacyclododecane-1,4,7-tri-tert-butyl-1,4,7,10-tetraazacyclododecane-1,4,7,10-tetraacetate (**5**).* 2-[4,7,10-Tris(2-*tert*-butoxy-2-oxoethyl)-1,4,7,10-tetraazacyclododecan-1-yl]acetic acid (**4**; 200 mg, 0.35 mmol; see the SI for synthesis), *N*,*N*′-dicyclohexylcarbodiimide (72 mg, 0.35 mmol), and *N*-hydroxysuccinimide (40 mg, 0.35 mmol) were dissolved in dichloromethane (DCM; 8 mL) and *N*,*N*-dimethylmethanamide (0.1 mL) and left to stir at room temperature overnight. After removal of the urea by filtration, the primary amine **3** (185 mg, 0.35 mmol) was added, and the reaction mixture was left to stir for 24 h. Concentration of the reaction mixture in vacuo and purification by silica gel chromatography (3% methanol/DCM; R_f = 0.3) gave the desired product as a white solid (200 mg, 53%). ^{1}H NMR ($CDCl_3$): δ 1.42 (s, 36H), 1.43 (s, 18H), 1.51 (bm, 2H), 2.32−2.71 (bm, 16H) 2.71−3.12 (bm, 8H), 3.14 (bs, 4H), 3.29−3.35 (bm, 12H), 3.50 (bs, 4H). ^{13}C NMR ($CDCl_3$): δ 27.8, 27.9, 28.5, 28.6, 31.4, 36.5, 48.0, 50.5, 74.4, 77.4, 81.7, 81.9, 162.7, 171.5, 172.3, 172.7. IR (ATR): 3443, 2974, 2931, 1721, 1684, 1365, 1225, 1154, 1105 cm^{-1}. LRMS (ESI). Calcd for $[M + Na]^+$: m/z 1106.7 (100%), 1084.7 (20%). HRMS (ESI). Calcd for $[M + Na]^+$: m/z 1106.7417. Found: m/z 1106.7417.

*2,2′,2″-[10-[2-[[3-(1,4,7,10-Tetraazacyclododecan-1-yl)propyl]-amino]-2-oxoethyl]-1,4,7,10-tetraazacyclododecane-1,4,7-triyl]-triacetic Acid, Trifluoroacetate Salt (**1**).* The Boc-protected amine **5** (64 mg, 0.059 mmol) was dissolved in DCM (2 mL), and TFA (0.3 mL) was added dropwise. After the solution was left to stir for 24 h, the solvent evaporated in vacuo, followed by the addition and removal of methanol (3 × 5 mL). The title compound was purified via preparative HPLC, and the fractions were analyzed via ^{1}H NMR spectroscopy and liquid chromatography−mass spectrometry. Pure fractions were combined and concentrated, yielding the product as the TFA salt [24 mg, 40%, based on tetrakis(trifluoroacetate salt)]. ^{1}H NMR (D_2O, 600 MHz): δ 1.77 (bp, J = 7.7 Hz, 2H), 2.78 (bt, J = 8.0 Hz, 2H), 2.99 (bs, 4H), 3.04 (bs, 4H), 3.15−3.21 (complex, 14H), 3.21−3.30 (complex, 12H), 3.60−4.00 (complex, 8H). ^{13}C NMR (D_2O, 150 MHz): δ 23.2 (b), 37.2 (b), 42.0 (b), 43.8 (b), 48.1 (b), 48.8 (b), 50.1 (b), 55.1 (b), 116.3 (q, J = 289 Hz), 163.0 (q, J = 35.6 Hz). LRMS (ESI). Calcd for $[M + H]^{2+}$: m/z 308.7 (100%), 616.4 (32%). Calcd for $[M + K]^+$: m/z 654.4 (30%). HRMS (ESI). Calcd for $[M + H]^+$: m/z 616.4068. Found: m/z 616.4139.

*Terbium(III) [10-(Propylamino)-1,4,7,10-tetraazacyclododecane-1,4,7-triacetato(3-)-κN^1,κN^4,κN^7,κN^{10},κO^1,κO^4,κO^7], Bis-(trifluoroacetate) Salt (Tb-**1**).* Ligand **1** (8 mg, 0.008 mmol) was dissolved in H_2O (0.5 mL), and the pH was adjusted to 8 using 0.25 M NaOH(aq). $Tb(OTf)_3$ (8 mg, 0.013 mmol) was dissolved in H_2O (0.5 mL) and added dropwise. The solution was heated to 50 °C, left to stir for 24 h, and monitored by ESI-MS. The reaction mixture was then filtered through a 0.2 μm syringe filter and purified via preparative HPLC. Fractions were analyzed via ESI-MS, and fractions containing the pure complex were combined and lyophilized to give the complex Tb-**1** as a white solid [7 mg, 91% based on bis(trifluoroacetate salt)]. NMR analysis was not performed on the terbium complex because of its paramagnetic nature. LRMS (ESI). Calcd for $[M + H]^{2+}$: m/z 386.6 (100%). Calcd for $[M + H]^+$: m/z 772.3 (80%). HRMS (ESI). Calcd for $[M + H]^+$: m/z 772.3120. Found: m/z 772.3138.

Luminescent Studies. *In Situ Preparation of a Solution of Tb-**1** + Lumazine.* Tb-**1** + lumazine was prepared by combining equal volumes of aqueous stock solutions of 1 mM Tb-**1**, TFA, and 1 mM lumazine. Solutions were incubated at 22 °C for 2 min prior to dilution to the appropriate concentration with a HEPES buffer (final HEPES concentration = 10 mM, pH 7.4). Solutions were then incubated at 22 °C for 10 min prior to use.

*LoD of Zinc(II) Using **Tb-1** + Lumazine.* Solutions of Tb-**1** + lumazine (20 μM) in a 10 mM HEPES buffer (pH 7.4) were incrementally spiked with a standard solution of $Zn(NO_3)_2{\cdot}6H_2O$ over the concentration of range of 0−40 μM, with the time-delayed luminescence emission at 545 nm recorded after each addition (λ_{ex}= 325 nm). From the measured data, the LoD was calculated from the linear range of the curve (0−18 μM) using 3sB/sensitivity, where sB corresponds to the standard deviation of the blank and the sensitivity is the slope of the least-squares linear-fitted luminescence signal versus $[Zn^{2+}]$ calibration curve (r^2 = 0.9786).[40,41]

Determination of Bound Metal-Inner-Sphere Water Molecules (q). The phosphorescence lifetimes of the Tb ($^5D_0$) excited state were measured in both H_2O and D_2O in the time-resolved mode at 298 K for solutions containing 20 μM Tb-**1** + lumazine and 1 equiv of Zn^{2+}. Lifetime values were obtained by monitoring the emission decay at 545 nm from the average of five independent measurements. All spectra were analyzed and fitted with a monoexponential function to give the rate constants of Tb-**1**·lumazine·Zn^{2+} in H_2O and D_2O, respectively (k_{O-H} and k_{O-D}). The number of water molecules bound directly to the metal inner sphere (q) was calculated according to

$$q^{Tb^{III}} = A'\Delta k_{corr}$$

$$\Delta k_{corr} = (k_{H_2O} - k_{D_2O}) - 0.06$$

where A' = 5 ms^{-1} for terbium,[30] k_{H_2O} = 0.57 ms^{-1}, k_{D_2O} = 0.30 ms^{-1}, and q = 1.04.

Luminescence Titrations and Estimation of the Binding Constants. Time-gated luminescence spectra of solutions of Tb-**1** + lumazine (5 or 20 μM) were measured separately in the presence of 0−13 μM Zn^{2+} (5 μM Tb-**1** + 5 μM lumazine) or 0−50 μM Zn^{2+} (20 μM Tb-**1** + 20 μM lumazine) in a 10 mM HEPES buffer (pH 7.4) with λ_{ex} = 325 nm and λ_{em} = 489, 545, 587, and 620 nm. Association constants were determined by fitting to binding models using a custom written python program *BindFit* available at www.supramolecular.org.[34] The raw data, calculated fit, and associated information can be accessed via the database through the links found in the SI.

Effect of Cations. The time-delayed luminescence emission enhancement of Tb-**1** + lumazine (20 μM) at 545 nm (λ_{ex} = 325 nm) was measured in a 10 mM HEPES buffer (pH 7.4) in the presence of 1.0 and 10.0 equiv of various cations. Metals (M) were added as NaI, $Hg(OAc)_2$, $Co(NO_3)_2$, $CaCl_2$, KCl, $Cu(NO_3)_2$, $MgCl_2$, $NiCl_2$, $Fe(NO_3)_2$, and $Cd(NO_3)_2$. The change in the luminescence of Tb-**1** + lumazine + M + Zn^{2+} was investigated by the subsequent addition of Zn^{2+} [1.0 equiv of $Zn(NO_3)_2{\cdot}6H_2O$] in both cases.

The time-delayed luminescence emission enhancement of Tb-**1** + lumazine + Zn^{2+} (5 μM) at 545 nm (λ_{ex} = 325 nm) was measured in a 10 mM HEPES buffer (pH 7.4) in the presence of 1.0 and 10.0 equiv of various cations. Metals were added as NaI, $Hg(OAc)_2$, $Co(NO_3)_2$, $CaCl_2$, KCl, $Cu(NO_3)_2$, $MgCl_2$, $NiCl_2$, $Fe(NO_3)_2$, and $Cd(NO_3)_2$.

■ ASSOCIATED CONTENT

Supporting Information

The Supporting Information is available free of charge on the ACS Publications website at DOI: 10.1021/acs.inorgchem.9b01771.

Supporting figures, links for the binding data fits, experimental procedures for synthesis of **4**, and NMR data (PDF)

DOI: 10.1021/acs.inorgchem.9b01771
Inorg. Chem. XXXX, XXX, XXX−XXX

AUTHOR INFORMATION

Corresponding Author

*E-mail: Kellie.Tuck@monash.edu. Web site: kellietuckgroup.com.

ORCID

Kellie L. Tuck: 0000-0002-9104-3158

Notes

The authors declare no competing financial interest.

ACKNOWLEDGMENTS

The authors acknowledge support from the School of Chemistry, Monash University.

REFERENCES

(1) Aulsebrook, M. L.; Graham, B.; Grace, M. R.; Tuck, K. L. Lanthanide complexes for luminescence-based sensing of low molecular weight analytes. *Coord. Chem. Rev.* **2018**, *375*, 191−220.

(2) Thibon, A.; Pierre, V. C. Principles of responsive lanthanide-based luminescent probes for cellular imaging. *Anal. Bioanal. Chem.* **2009**, *394*, 107−20.

(3) Shuvaev, S.; Starck, M.; Parker, D. Responsive, water-soluble europium(III) luminescent probes. *Chem. - Eur. J.* **2017**, *23*, 9974−9989.

(4) Butler, S. J.; Parker, D. Anion binding in water at lanthanide centres: from structure and selectivity to signalling and sensing. *Chem. Soc. Rev.* **2013**, *42*, 1652−1666.

(5) Aletti, A. B.; Gillen, D. M.; Gunnlaugsson, T. Luminescent/colorimetric probes and (chemo-) sensors for detecting anions based on transition and lanthanide ion receptor/binding complexes. *Coord. Chem. Rev.* **2018**, *354*, 98−120.

(6) Sabbatini, N.; Guardigli, M.; Lehn, J. M. Luminescent lanthanide complexes as photochemical supramolecular devices. *Coord. Chem. Rev.* **1993**, *123*, 201.

(7) Beeby, A.; Faulkner, S.; Parker, D.; Williams, J. G. Sensitised luminescence from phenanthridine appended lanthanide complexes: analysis of triplet mediated energy transfer processes in terbium, europium and neodymium complexes. *J. Chem. Soc., Perkin Trans. 2* **2001**, *8*, 1268−1273.

(8) Evans, C. H. *Biochemistry of the Lanthanides*; Springer Science & Business Media, 2013; Vol. *8*.

(9) Gschneidner, K. A.; Bünzli, J.-C. G.; Pecharsky, V. K. *Handbook on the physics and chemistry of rare earths: optical spectroscopy*; Elsevier, 2011; Vol. *37*.

(10) Hu, W.; Bai, F.; Gong, X.; Zhan, X.; Fu, H.; Bjornholm, T. *Organic optoelectronics*; John Wiley & Sons, 2012.

(11) Samuel, A. P. S. *Optimizing new classes of luminescent lanthanide complexes*; ProQuest, 2008.

(12) Aulsebrook, M. L.; Graham, B.; Grace, M. R.; Tuck, K. L. The synthesis of luminescent lanthanide-based chemosensors for the detection of zinc ions. *Tetrahedron* **2014**, *70*, 4367−4372.

(13) Thorson, M. K.; Ung, P.; Leaver, F. M.; Corbin, T. S.; Tuck, K. L.; Graham, B.; Barrios, A. M. Lanthanide complexes as luminogenic probes to measure sulfide levels in industrial samples. *Anal. Chim. Acta* **2015**, *896*, 160−165.

(14) O'Malley, W. I.; Abdelkader, E. H.; Aulsebrook, M. L.; Rubbiani, R.; Loh, C.-T.; Grace, M. R.; Spiccia, L.; Gasser, G.; Otting, G.; Tuck, K. L.; Graham, B. Luminescent alkyne-bearing terbium (III) complexes and their application to bioorthogonal protein labeling. *Inorg. Chem.* **2016**, *55*, 1674−1682.

(15) O'Malley, W. I.; Rubbiani, R.; Aulsebrook, M. L.; Grace, M. R.; Spiccia, L.; Tuck, K. L.; Gasser, G.; Graham, B. Cellular uptake and photo-cytotoxicity of a gadolinium(III)-DOTA-naphthalimide complex "clicked" to a lipidated tat peptide. *Molecules* **2016**, *21*, 194.

(16) Aulsebrook, M. L.; Biswas, S.; Leaver, F. M.; Grace, M. R.; Graham, B.; Barrios, A. M.; Tuck, K. L. A luminogenic lanthanide-based probe for the highly selective detection of nanomolar sulfide levels in aqueous samples. *Chem. Commun.* **2017**, *53*, 4911−4914.

(17) Loh, C.-T.; Graham, B.; Abdelkader, E. H.; Tuck, K. L.; Otting, G. Generation of pseudocontact shifts in proteins with lanthanides using small "clickable" nitrilotriacetic acid and iminodiacetic acid tags. *Chem. - Eur. J.* **2015**, *21*, 5084−5092.

(18) Loh, C. T.; Ozawa, K.; Tuck, K. L.; Barlow, N.; Huber, T.; Otting, G.; Graham, B. Lanthanide tags for site-specific ligation to an unnatural amino acid and generation of pseudocontact shifts in proteins. *Bioconjugate Chem.* **2013**, *24*, 260−268.

(19) Aulsebrook, M. L.; Starck, M.; Grace, M. R.; Graham, B.; Thordarson, P.; Pal, R.; Tuck, K. L. Interaction of nucleotides with a trinuclear terbium(III)-dizinc(II) complex: efficient sensitization of terbium luminescence by guanosine monophosphate and application to real-time monitoring of phosphodiesterase activity. *Inorg. Chem.* **2019**, *58*, 495−505.

(20) (a) Isaac, M.; Raibaut, L.; Cepeda, C.; Roux, A.; Boturyn, D.; Eliseeva, S. V.; Petoud, S.; Sénèque, O. Luminescent zinc fingers: Zn-responsive neodymium near-infrared emission in water. *Chem. - Eur. J.* **2017**, *23*, 10992−10996. (b) Isaac, M.; Pallier, A.; Szeremeta, F.; Bayle, P.-A.; Barantin, L.; Bonnet, C. S.; Sénèque, O. MRI and luminescence detection of Zn2+ with a lanthanide complex-zinc finger peptide conjugate. *Chem. Commun.* **2018**, *54*, 7350−7353. (c) Gunnlaugsson, T.; Harte, A. J.; Leonard, J. P.; Nieuwenhuyzen, M. The Formation of Luminescent Supramolecular Ternary Complexes in Water: Delayed Luminescence Sensing of Aromatic Carboxylates Using Coordinated Unsaturated Cationic Heptadentate Lanthanide Ion Complexes. *Supramol. Chem.* **2003**, *15*, 505−519. (d) Esplin, T. L.; Cable, M. L.; Gray, H. B.; Ponce, A. Terbium-Macrocycle Complexes as Chemical Sensors: Detection of an Aspirin Metabolite in Urine Using a Salicylurate-Specific Receptor Site. *Inorg. Chem.* **2010**, *49*, 4643−4647.

(21) Lee, A. E.; Grace, M. R.; Meyer, A. G.; Tuck, K. L. Fluorescent Zn2+ chemosensors, functional in aqueous solution under environmentally relevant conditions. *Tetrahedron Lett.* **2010**, *51*, 1161−1165.

(22) Aulsebrook, M. L.; Graham, B.; Grace, M. R.; Tuck, K. L. Coumarin-based fluorescent sensors for zinc(II) and hypochlorite. *Supramol. Chem.* **2015**, *27*, 798−806.

(23) Vallee, B. L.; Falchuk, K. H. The biochemical basis of zinc physiology. *Physiol. Rev.* **1993**, *73*, 79−118.

(24) Ye, Z.; Xiao, Y.; Song, B.; Yuan, J. Design and synthesis of a new terbium complex-based luminescent probe for time-resolved luminescence sensing of zinc ions. *J. Fluoresc.* **2014**, *24*, 1537−1544.

(25) Ye, Z.; Wang, G.; Chen, J.; Fu, X.; Zhang, W.; Yuan, J. Development of a novel terbium chelate-based luminescent chemosensor for time-resolved luminescence detection of intracellular Zn2+ ions. *Biosens. Bioelectron.* **2010**, *26*, 1043−1048.

(26) Roger, M.; Regueiro-Figueroa, M.; Ben Azzeddine, C.; Patinec, V.; Bonnet, C. S.; Platas-Iglesias, C.; Tripier, R. Lanthanide complexes with heteroditopic ligands as fluorescent zinc sensors. *Eur. J. Inorg. Chem.* **2014**, *2014*, 1072−1081.

(27) Comby, S.; Tuck, S. A.; Truman, L. K.; Kotova, O.; Gunnlaugsson, T. New trick for an old ligand! The sensing of Zn(II) using a lanthanide based ternary Yb(III)-cyclen-8-hydroxyquinoline system as a dual emissive probe for displacement assay. *Inorg. Chem.* **2012**, *51*, 10158−10168.

(28) Matsubara, T.; Hirao, K. Density functional study of the binding of the cyclen-coordinated M (II)(M= Zn, Cu, Ni) complexes to the DNA base. Why is Zn better to bind? *J. Mol. Struct.: THEOCHEM* **2002**, *581*, 203−213.

(29) Han, M. S.; Kim, D. H. Readily available fluorescence probes for zinc ion in aqueous solution of neutral pH. *Supramol. Chem.* **2003**, *15*, 59−64.

(30) Beeby, A.; Clarkson, I. M.; Dickins, R. S.; Faulkner, S.; Parker, D.; Royle, L.; de Sousa, A. S.; Williams, J. A. G.; Woods, M. Non-radiative deactivation of the excited states of europium, terbium and ytterbium complexes by proximate energy-matched OH, NH and CH oscillators: an improved luminescence method for establishing solution hydration states. *J. Chem. Soc., Perkin Trans. 2* **1999**, *3*, 493−504.

DOI: 10.1021/acs.inorgchem.9b01771
Inorg. Chem. XXXX, XXX, XXX−XXX

(31) Thordarson, P. Determining association constants from titration experiments in supramolecular chemistry. *Chem. Soc. Rev.* **2011**, *40*, 1305−1323.
(32) Ulatowski, F.; Dąbrowa, K.; Bałakier, T.; Jurczak, J. Recognizing the limited applicability of Job plots in studying host-guest interactions in supramolecular chemistry. *J. Org. Chem.* **2016**, *81*, 1746−1756.
(33) Brynn Hibbert, D.; Thordarson, P. The death of the Job plot, transparency, open science and online tools, uncertainty estimation methods and other developments in supramolecular chemistry data analysis. *Chem. Commun.* **2016**, *52*, 12792−12805.
(34) http://supramolecular.org, accessed March 13, 2019.
(35) Kimura, E.; Aoki, S.; Koike, T.; Shiro, M. A Tris(ZnII-1,4,7,10-tetraazacyclododecane) Complex as a New Receptor for Phosphate Dianions in Aqueous Solution. *J. Am. Chem. Soc.* **1997**, *119*, 3068−3076.
(36) Bhuyan, M.; Katayev, E.; Stadlbauer, S.; Nonaka, H.; Ojida, A.; Hamachi, I.; König, B. Rigid Luminescent Bis-Zinc(II)-Bis-Cyclen Complexes for the Detection of Phosphate Anions and Non-Covalent Protein Labeling in Aqueous Solution. *Eur. J. Org. Chem.* **2011**, *2011* (15), 2807−2817.
(37) National Recommended Water Quality Criteria - Aquatic Life Criteria TablelWater Quality CriterialU.S. EPA, https://www.epa.gov/wqc/national-recommended-water-quality-criteria-aquatic-life-criteria-table, accessed March 13, 2019.
(38) Woods, M.; Kiefer, G. E.; Bott, S.; Castillo-Muzquiz, A.; Eshelbrenner, C.; Michaudet, L.; McMillan, K.; Mudigunda, S. D.; Ogrin, D.; Tircsó, G.; Zhang, S.; Zhao, P.; Sherry, A. D. Synthesis, relaxometric and photophysical properties of a new pH-responsive MRI contrast agent: The effect of other ligating groups on dissociation of ap-nitrophenolic pendant arm. *J. Am. Chem. Soc.* **2004**, *126*, 9248−9256.
(39) Kamaly, N.; Kalber, T.; Ahmad, A.; Oliver, M. H.; So, P.-W.; Herlihy, A. H.; Bell, J. D.; Jorgensen, M. R.; Miller, A. D. Bimodal paramagnetic and fluorescent liposomes for cellular and tumor magnetic resonance imaging. *Bioconjugate Chem.* **2008**, *19*, 118−129.
(40) Miller, J. C.; Miller, J. N. *Statistics for Analytical Chemistry*, 2nd ed.; U.S. Department of Energy, 1988.
(41) Skoog, D. A.; Holler, F.; Nieman, T. *Principles of Instrumental Analysis*, 5th ed.; Harcourt Asia Pte, Ltd., 1992.

DOI: 10.1021/acs.inorgchem.9b01771
Inorg. Chem. XXXX, XXX, XXX−XXX